Thermal and Rheological Properties of Crude Tall Oil for Use in Biodiesel Production

Peter Adewale and Lew P. Christopher *

Biorefining Research Institute, Lakehead University, 1294 Balmoral Street, Thunder Bay, ON P7B 5E1, Canada; padewale@lakeheadu.ca

* Correspondence: lchristo@lakeheadu.ca; Tel.: +1-807-343-8844

Abstract: The primary objective of this work was to investigate the thermal and rheological properties of crude tall oil (CTO), a low-cost by-product from the Kraft pulping process, as a potential feedstock for biodiesel production. Adequate knowledge of CTO properties is a prerequisite for the optimal design of a cost-effective biodiesel process and related processing equipment. The study revealed the correlation between the physicochemical properties, thermal, and rheological behavior of CTO. It was established that the trans/esterification temperature for CTO was greater than the temperature at which viscosity of CTO entered a steady-state. This information is useful in the selection of appropriate agitation conditions for optimal biodiesel production from CTO. The point of interception of storage modulus (G′) and loss modulus (G″) determined the glass transition temperature (40 °C) of CTO that strongly correlated with its melting point (35.3 °C). The flow pattern of CTO was modeled as a non-Newtonian fluid. Furthermore, due to the high content of fatty acids (FA) in CTO, it is recommended to first reduce the FA level by acid catalyzed methanolysis prior to alkali treatment, or alternatively apply a one-step heterogeneous or enzymatic trans/esterification of CTO for high-yield biodiesel production.

Keywords: crude tall oil; crystallization; melting; viscosity; biodiesel

1. Introduction

Due to the increasing offshore completion, fluctuating oil prices and demand for green and environmentally-friendly technologies, the North American pulp and paper industry needs to increase its revenues and competitiveness through valorization of waste streams, product and market diversification. One such opportunity is presented by crude tall oil (CTO), a by-product from the Kraft pulping process, that is currently sold by most pulp and paper mills to chemical companies for further processing to value-added products. CTO contains a wide range of constituents including light oil, fatty acids (FA), rosin acids (RA), distilled tall oil, pitch residue, and neutral components such as sterols and triglycerides (TGs). The type of wood species (predominantly softwood) used in the pulping process is a factor which determines the yield and composition of CTO, including its fatty and rosin acids content [1,2]. Other factors that affect the properties of CTO include geographical location, type and length of wood storage, hardwood and wood residue usage in chemical pulping, and season of the year [3,4].

The prospect and potential of CTO for production of value-added, bio-based chemicals and biofuels has been identified by many researchers [2]. CTO has been investigated for production of adhesives [5], paints [6], rubber [7,8], coatings [9,10], biodiesel [11,12], paraffin-rich liquids [13], diesel fuel additives [14], ethylene and propylene [15], etc. A better understanding and information on the thermal and rheological properties of CTO such as viscosity, melting and crystallization are essential engineering parameters for the optimal design of processing equipment and optimization of production methods based on CTO. The FA composition, including the saturated fatty acids (SFA)

fraction, contained in biodiesel feedstocks such as CTO, animal fats, and vegetable oils is responsible for the hardness, viscoelasticity and plasticity of these raw materials [16–18]. The analysis and quantification of these properties can be used to predict the optimal processing variations or to modify the processing equipment for more efficient operation.

Several studies have been carried out on the rheological, thermal and physicochemical properties of biodiesel feedstocks including animal fats, vegetable oils, blends, and shortening [19–23]. In a comprehensive review on feedstocks used for biodiesel production, Karmakar et al. [17] reported that animal fats have chemical structures similar to vegetable oils, with the only difference being the FA distribution profile. The effect of catalyst, free fatty acids (FFA), and water on transesterification of edible beef tallow was studied by Ma et al. [24] who established that the FFA and water content should be kept within 0.06% and 0.5% w/w, respectively, in order to attain a maximal biodiesel yield. CTO was assessed as a feedstock for production of renewable bioethylene, biopropylene, and bioaromatics [15]. Balo [25] reported that highly-epoxidized tall oil significantly improved the thermal conductivity and density of sample mixtures tested as green insulation materials. Jenab et al. [2] demonstrated the feasibility of producing renewable hydrocarbons through pyrolysis of the FA-rich distillate fraction of CTO. Similarly, Coll et al. [14] described an economically-viable process for conversion of the RA fraction of CTO to fuels (gasoline and diesel) and chemicals (fuel additives). A biodiesel yield of 70% was obtained through heterogeneous acid-catalyzed transesterification of CTO under the following optimal conditions: reaction temperature of 250 °C; methanol to CTO molar ratio of 10; reaction time of 4 h; catalyst amount of 3% w/w; and stirring intensity of 625 rpm [11].

Despite the widely reported acceptance and suitability of CTO to serve as a viable feedstock for biochemicals and biofuels production, limited attention has been given to the rheological (viscosity) and thermal (melting, crystallization) properties of CTO in the literature. For example, viscosity is an important factor in biodiesel production from CTO in accordance with the American Standard Test Methods (ASTM) [11,26,27]. In an investigation of the kinematic viscosity of CTO-derived biodiesel, Mkhize et al. [11] reported a significant 53-fold reduction of viscosity, from 344.1 cP (CTO) to 6.5 cP (biodiesel). This information has been adequately used to improve the fuel automation in the combustion chamber of the biodiesel engine [26]. For the design and optimization of production systems based on CTO, it is of paramount importance to obtain comprehensive knowledge and understanding of the rheo-thermal behavior of CTO, which is currently lacking in literature. Furthermore, the suitability of CTO for synthesis of biodiesel with desired properties requires a systematic study of the influence of FA composition on CTO thermal and rheological properties. Hence, the objective of this study was to investigate the thermal and rheological properties of CTO as a low-cost and currently underutilized feedstock for biodiesel production.

2. Materials and Methods

2.1. Materials

CTO was obtained from a pulp and paper mill in Canada. The CTO sample was kept in a refrigerator at a temperature below 4 °C until use. Hexane (ACS grade), chloroform, sodium thiosulphate, potassium iodide, sodium hydroxide, WIJS solution, and sulfuric acid (99.9%) were purchased from Fisher Scientific (Nepean, ON, Canada). Saturated and unsaturated fatty acid methyl ester (FAME) and FFA standards were purchased from Sigma-Aldrich (Oakville, ON, Canada).

2.2. Rheological Analyses

Viscoelasticity and viscosity measurements of CTO samples were carried out using a Discovery Hybrid Rheometer HR-2 (TA Instruments, New Castle, DE, USA). Samples were placed in the 1 mm gap between two stainless steel parallel plates (plate diameter 40 mm). The sample temperature was controlled by the rheometer's Peltier cooling system and monitored with platinum resistance thermometer sensors (accuracy of ±0.1 °C). The instrument was set at zero-gap before the actual

measurement. Oscillatory temperature ramps were carried out to determine the temperature dependence of viscosity, melting strength and the viscoelastic behavior while a controlled stress-rotation shear rate ramp method was used to investigate viscosity. The sample temperature was equilibrated at 30 °C for 5 min before the test. An initial pre-shear stress of 0.5968 Pa was found to produce a response within the linear viscoelastic region (LVR) of each test sample at a fixed frequency of 1 Hz. A temperature ramp of 30–60 °C was performed at a ramp rate of 5 °C/min by loading the sample onto the rheometer plate to fill up the space between the geometry and the plate. Frequency sweep tests (0.1–10 Hz) were carried out within the LVR at constant shear stress (0.5 Pa) and 0.1–10 Hz. A fresh set of samples was isothermally heated up to 60 °C and held for 20 min at that temperature, and then rapidly cooled to 30 °C, before the frequency sweep tests started. Viscosity analysis was carried out on a different sample set. The instrument was programmed to a fixed temperature (30, 40, 50 and 60 °C) and equilibrated for 10 min followed by one-cycle shear rate ramping from 50 to 250 s^{-1}. Viscosity behavior over the range of shear rate ramping of CTO was investigated at different temperatures (30, 40, 50 and 60 °C) in order to identify conditions that favor enzymatic transesterification. The storage modulus (G′) and loss modulus (G″) of CTO were determined as a function of temperature and frequency. The viscosity and viscoelastic measurements were carried out in duplicate. The rheological parameters were obtained by direct integration of the rheograms and the best-fitted curve; the flow models were fitted to the resultant curves using the manufacturer's supplied computer software (TRIOS, TA Instruments, New Castle, DE, USA).

2.3. Thermal Analysis by Differential Scanning Calorimeter (DSC)

Heat capacity, melting, and crystallization curves of CTO were determined using DSC (Q 2000, TA Instrument, New Castle, DE, USA). Purge gas was nitrogen (99.99% purity) with a flow rate of 50 mL/min. The instrument was calibrated using indium (melting point of 156.6 °C; enthalpy ΔH_f of 28.45 J/g). The CTO samples (15–20 mg) were transferred into aluminum hermetic pans and the covers of the pans were hermetically sealed. An empty, hermetically-sealed aluminum pan was used as a reference. The baseline was optimized using two empty pans (one placed at the reference oven compartment, and the other at the sample oven compartment) prior to sample analysis. To examine the crystallization characteristics of CTO, samples were subjected to the following temperature program: (a) heated to 80 °C to destroy any crystal structures; (b) equilibrated at 80 °C for 1 min; (c) held isothermally for 9 min; and (d) ramped at a rate of 10 °C/min from 80 to −40 °C. The melting characteristics of CTO were studied using a fresh sample set subjected to: (a) cooling to −40 °C; (b) equilibrating at −40 °C for 1 min; (c) holding isothermally at −40 °C for 9 min; and (d) ramping at a rate of 10 °C/min from −40 to 80 °C. For specific heat capacity, a temperature protocol module was used with the following temperature program: (a) cooling to −40 °C; (b) equilibrating at −40 °C for 1 min; (c) holding isothermally at −40 °C for 9 min; and (d) ramping at a rate of 10 °C/min from −40 to 80 °C. The crystallization and melting characteristics of each sample, i.e., extrapolated onset temperature (T_{onset}), maximum peak temperature (T_{peak}) and enthalpy (ΔH), were obtained using TA Universal Analysis 2000 software (Q 2000, TA Instrument, New Castle, DE, USA). Data were collected and analyzed in duplicate.

2.4. Physicochemical Properties

The physicochemical properties, including ash content (AC), resin acid (RA), unsaponifiable matter (USM), iodine value (IV), saponification number (SN), acid number (AN), and free fatty acid (FFA)) of CTO were determined according to ASTM standard methods. FA identification and quantification was carried out using a GC model (Trace 1300, Thermo Scientific, Chicago, IL, USA) equipped with an autosampler and a flame ionized detector (FID). The relative retention time of each FFA was compared to that of the FFA standards. Standard calibration curves were developed for FFA identification and quantification. The repeatability (within-run precision) and reproducibility (between-run precision) were carried out on four different standards to validate the GC-FID accuracy.

2.5. Statistical Analysis

Statistical analysis was carried out according to the general linear model procedure (PROC GLM) using SAS (Statistical Analysis Systems, Version 9.4, SAS Institute Inc., Cary, NC, USA). The mean comparison of CTO viscosities at selected temperatures and the significant differences between the temperatures and shear rates were further analyzed with the Tukey's studentized range test. Tukey's honest significant difference (HSD) test is a single-step multiple comparison procedure that compares the means of every treatment to the means of every other treatment.

3. Results

3.1. Physicochemical Properties

A number of wood processing steps, from wood storage to chemical (kraft) pulping and CTO recovery from black liquor, can influence the properties of CTO (Figure 1). At room temperature, CTO is a tarlike substance with unpleasant and penetrating odor caused by sulfur-containing components present in the pulping liquor. As can be seen from Table 1, CTO contained a high percentage (53.4%) of FFA, with linoleic acid (C18:2n6) comprising 46.2% of the total FFA. The IV of CTO of 110.50 mg/gI_2 is indicative of a high percentage of unsaturated fatty acid (UFA) and low percentage SFA in CTO. The SN of CTO (150) appeared to be higher than the AN (130). The AC was very low (0.46%) which signifies a limited amount of inorganic matter in the sample. The total percentage of SFA and UFA in CTO were 7.23% and 77.12%, respectively, with a UFA/SFA ratio of 10.67. This value is high enough for the sample to be in liquid state at room temperature. As discussed above, many factors can impact on the CTO composition and properties, including its tarlike nature (Figure 1).
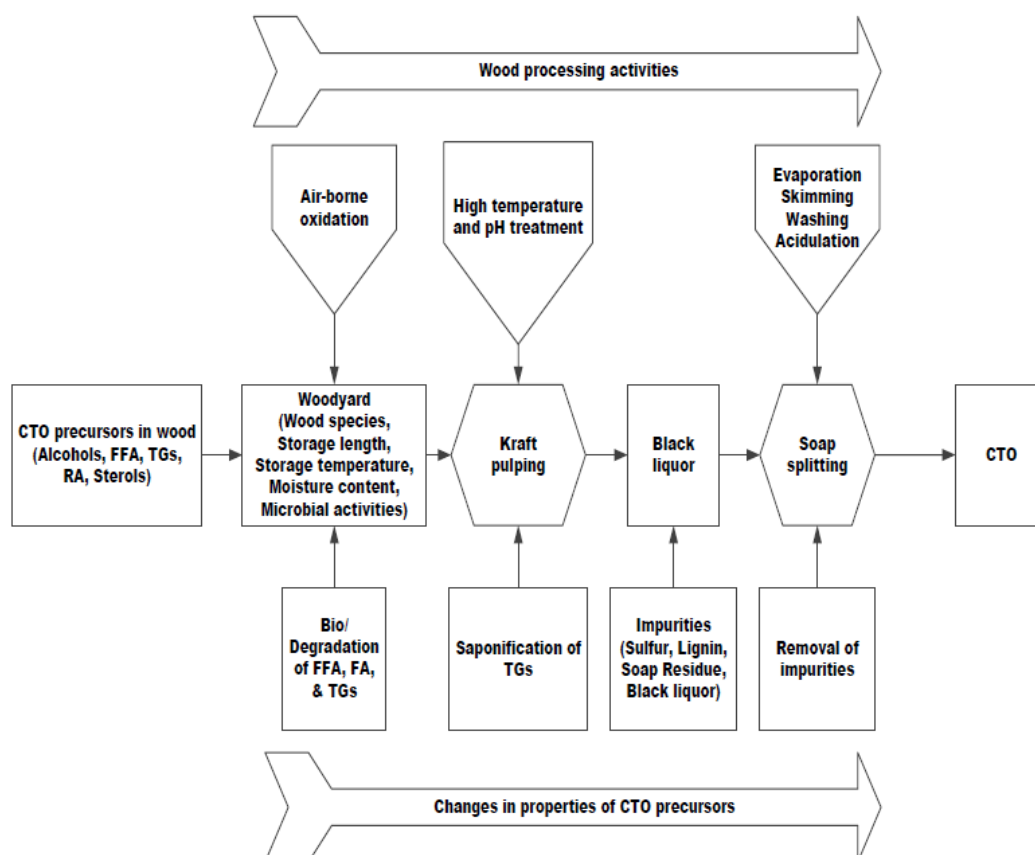

Figure 1. Modification of crude tall oil (CTO) precursors from wood handling to CTO recovery. Triglycerides (TGs), Resin acids (RAs), Free fatty acid (FFA), Fatty acid (FA).
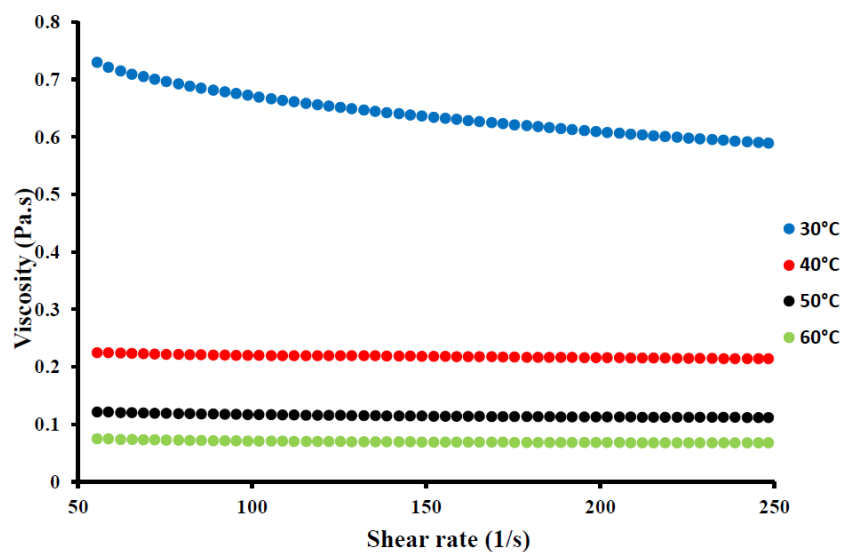
Table 1. CTO physicochemical properties.

CTO Analysis	Value
Free Fatty Acid Composition (%)	
C16:0	5.98 ± 0.14
C16:1	1.29 ± 0.08
C18:0	1.25 ± 0.12
C18:1	13.99 ± 0.18
C18:2n6	46.24 ± 0.21
γ-C18:3n6	6.48 ± 0.15
C18:3n3	1.58 ± 0.06
C20:2	3.46 ± 0.04
C20:3n6	2.57 ± 0.11
C20:4n6	1.51 ± 0.25
Unknown	11.44 ± 0.43
$\sum$SFA	7.23 ± 0.07
$\sum$UFA	77.12 ± 0.16
UFA/SFA ratio	10.67
Physicochemical Properties	
FFA (%)	53.36 ± 0.14
Water (%)	1.54 ± 0.02
AC (%)	0.46 ± 0.07
RA (%)	28.40 ± 0.95
USM (%)	16.70 ± 0.19
IV (mg/gI$_2$)	110.50 ± 0.31
SN (mg KOH/g CTO)	150.00 ± 4.30
AN (mg KOH/g CTO)	130.00 ± 0.54

% expressed on *w/w* basis. Ash content (AC), Resin acid (RA), Unsaponifiable matter (USM), Iodine value (IV), Saponification number (SN), Acid number (AN), Saturated fatty acid (SFA), Unsaturated fatty acid (UFA), Free fatty acid (FFA).

3.2. Rheological Properties—Linear Viscosity and Viscoelasticity of CTO

The viscosity–shear rate relationship for CTO was studied at four different temperatures (30, 40, 50, and 60 °C) and presented in Figure 2. The interaction between shear rate and temperature was significant ($p < 0.05$). Above 40 °C, however, the glass transition temperature of CTO was exceeded, which resulted in a steady-state viscosity over the shear rate range tested.

Figure 2. Impact of CTO temperature on the viscosity vs shear rate interaction.

The HSD mean comparison of the CTO viscosity in the 30–60 °C temperature range is displayed in Figure 3. The highest viscosity distribution was observed at 30 °C ($p < 0.05$). The Tukey's studentized range test revealed that all temperatures were significantly different ($p < 0.05$) from each other in their effect on CTO viscosity. Data on the rheological flow properties of CTO were obtained by linearly increasing the shear rate from 50 to 250 s^{-1}.
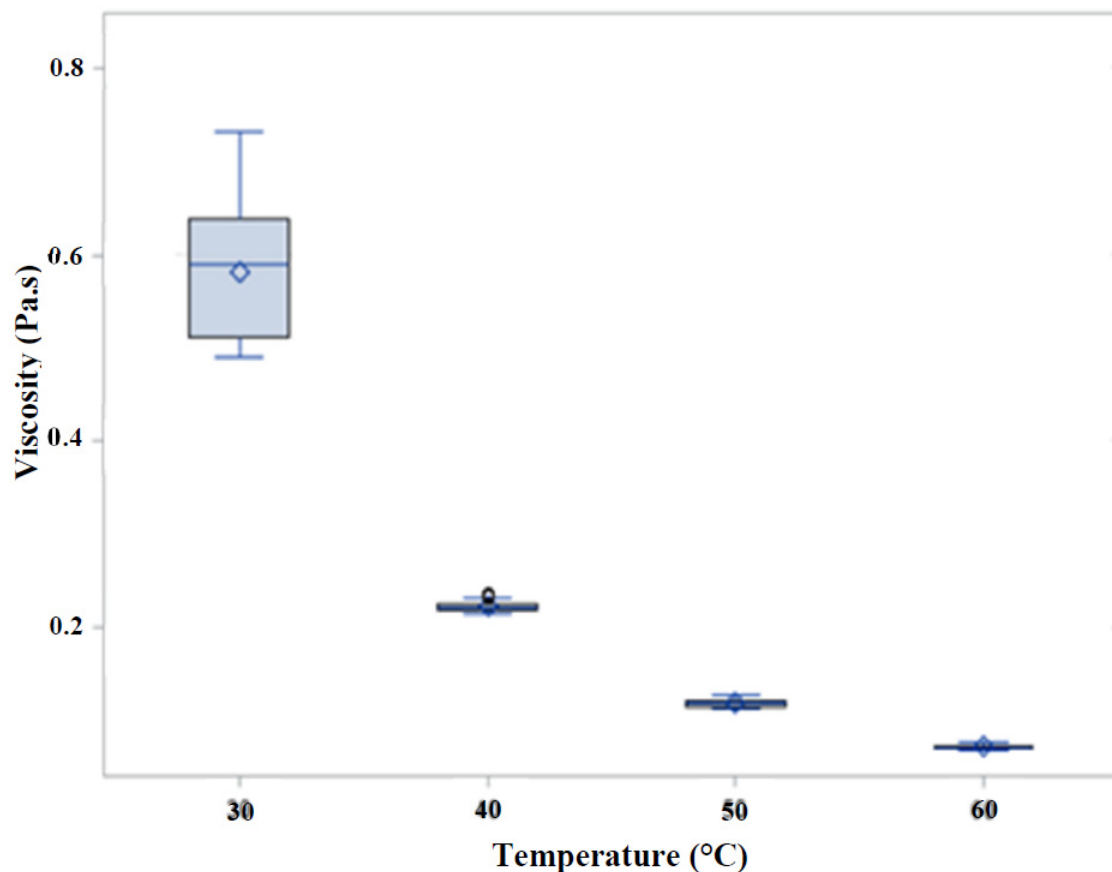

Figure 3. Impact of temperature on the viscosity distribution profile of CTO.

The flow curves were studied at different temperatures to illustrate the onset of non-Newtonian behavior. The temperature was ramped from 30 to 60 °C at 5 °C/min by loading the sample onto the rheometer plate to fill up the space between the geometry and the plate. The results were plotted in terms of shear stress vs shear rate (Figure 4). During the model analysis, five flow model types (Newtonian, Bingham, Casson, Power law, and Herschel–Bulkley) were fitted to the flow data. There was a wide gap between flow data of 30 °C and other temperatures (Figure 5). At 30 °C, the best-fitted model to the flow data was Herschel–Bulkley with a significant coefficient of determination $R^2 = 0.999994$, viscosity = 1.50 Pa.s, and rate index = 0.83. The same best-fitted model was observed for each of the temperatures investigated in this study. At 60 °C, the best-fitted model to the flow data was Herschel–Bulkley with a coefficient of determination $R^2 = 0.999998$, viscosity = 0.072 Pa.s, and rate index = 0.99. The results of the best-fitted flow model proved CTO as a non-Newtonian fluid within the temperatures range 30–60 °C. Further investigations were carried out to better understand the dynamic rheology of CTO.
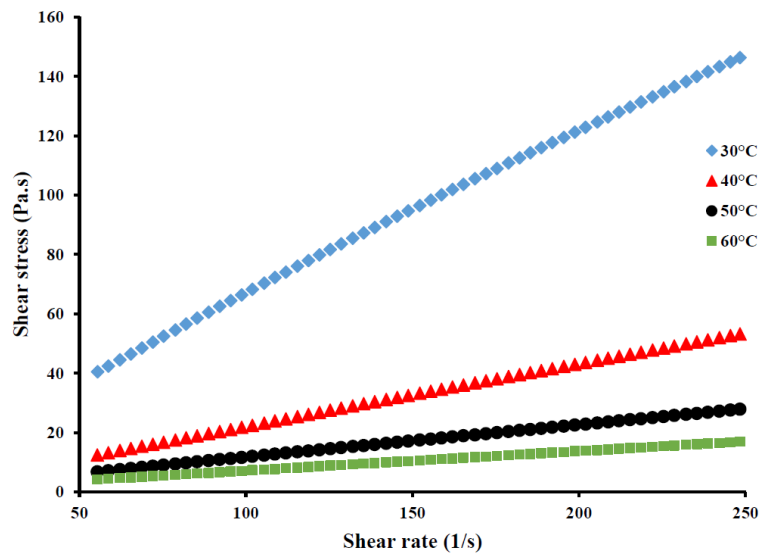
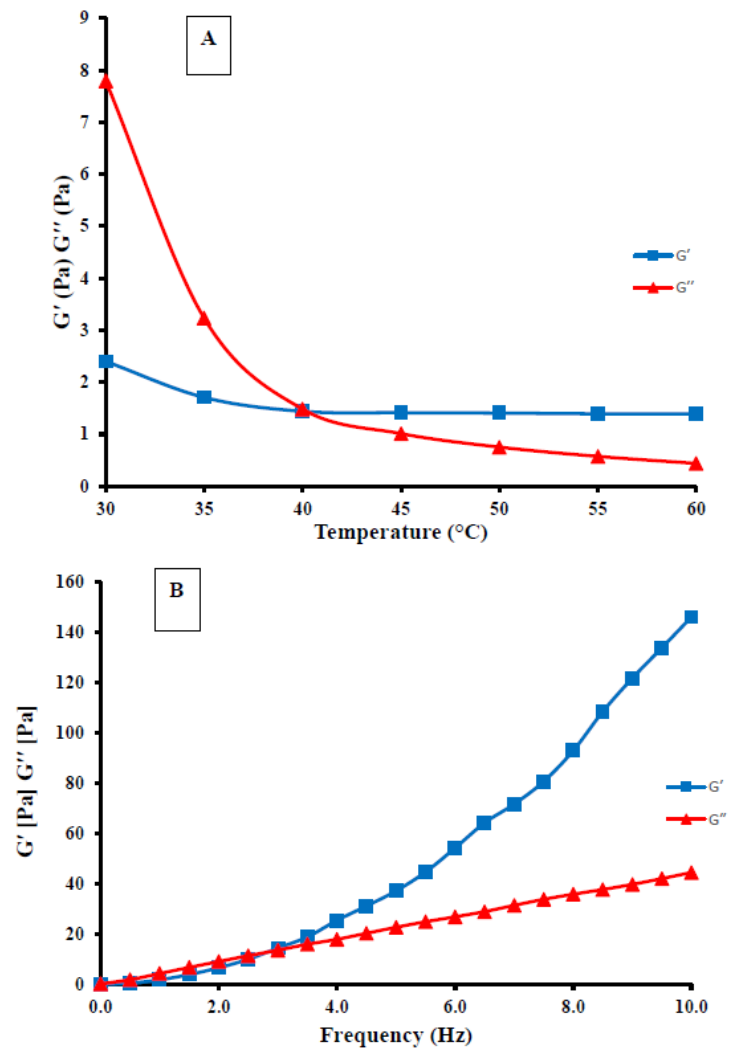**Figure 4.** Impact of temperature on the flow model curves of CTO.

Figure 5. Viscoelastic characterization of CTO changes in storage modulus (G′) and loss modulus (G″) (**A**) Temperature sweep (**B**) Frequency sweep.

The viscoelastic properties of CTO were evaluated through their storage modulus (G′) and loss modulus (G″), in which G′ relate to the elastic or solid behavior of the material while G″ represents the viscous or fluid behavior. The changes in the behavior of CTO's constituents were temperature-dependent, and consequently, the viscoelastic behavior of CTO was affected by the temperature variation. Figure 5A depicts the G′ and G″ values of CTO under a temperature sweep procedure. The intercepting point of G′ and G″ at 40 °C signified the glass transition temperature of CTO. Above these temperatures, the CTO sample showed a viscous behavioral pattern as presented in Figure 2. Frequency sweep tests (0.1–10 Hz) were carried out within the LVR, at a constant shear stress (0.5 Pa). Under a frequency sweep procedure (Figure 5B), CTO displayed higher G″ than G′ values, up to 3 Hz, beyond which G′ grew exponentially whereas G″ increased linearly up to the end of the run.

3.3. Thermal Characteristics of CTO

The melting and crystallization curves of CTO as determined by DSC are presented in Figure 6 A,B whereas Table 2 summarizes the melting and crystallization parameters of CTO, including onset temperature (T_{onset}), peak temperatures (T_{peak}), and enthalpy change (ΔH). As mentioned earlier, CTO is a mixture of long-chain FA (that differ in carbon chain length and degree of saturation), RA, and neutral products. From the melting profile of CTO (Figure 6A), the values of T_{onset} and T_{peak} were determined as 27.42 and 35.29 °C, respectively, while T_{onset} and T_{peak} from the CTO crystallization profile (Figure 6B) were 24.00 and 16.26 °C, respectively (Table 2). Specific heat capacity of CTO, measured with a modulated temperature protocol module of DSC, was determined to be 2.54 J/(g °C) at 34.33 °C.
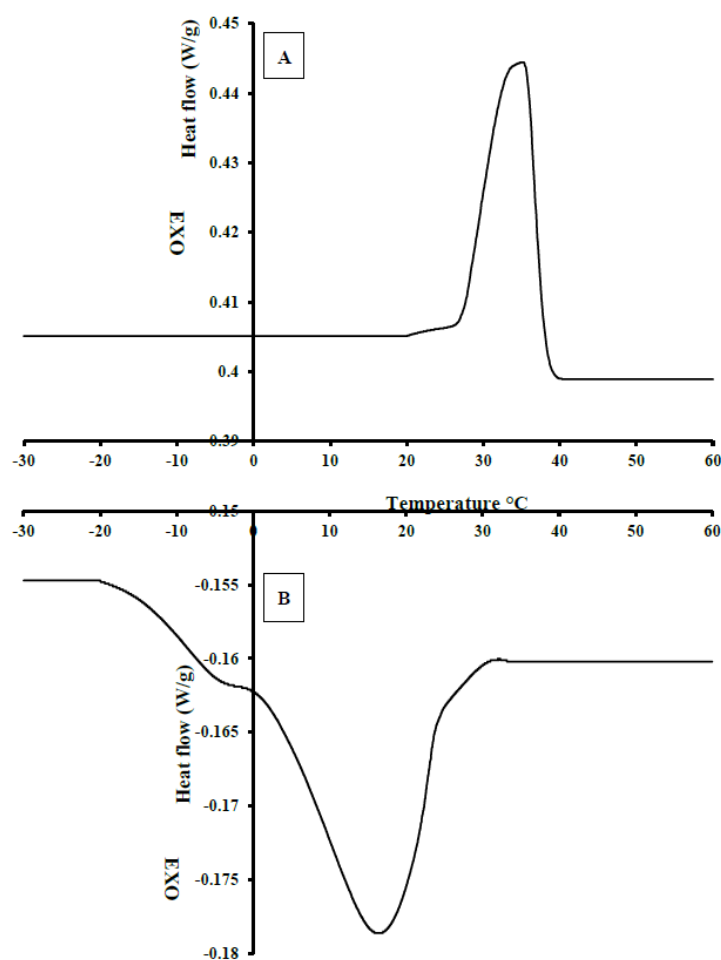

Figure 6. Differential scanning calorimeter (DSC) thermograms of CTO (**A**) Melting curve (**B**) Crystallization curve.

Table 2. T_{onset}, T_{peak} and ΔH values obtained from melting, crystallization and heat capacity of CTO.

Characteristics	T_{onset} (°C)	T_{peak} (°C)	ΔH (J/g)
Melting	27.42 ± 0.35	35.29 ± 0.54	1.73 ± 0.05
Crystallization	24.00 ± 0.13	16.73 ± 0.08	2.52 ± 0.22
Heat capacity	27.28 ± 0.22	34.33 ± 0.08	1.77 ± 0.25

4. Discussion

4.1. Physicochemical Properties of CTO

The amount of FFA in biodiesel feedstocks determines the method of choice for biodiesel production. The FFA content of CTO (53.4%) is much higher than the recommended value of below 1% for the use of alkaline catalysis, a common industrial method of biodiesel production [28,29]. Hence, the higher the quantity of FFA in the biodiesel feedstocks, the less suitable the standard alkaline transesterification method. Therefore, at high FFA content, enzymatic or heterogeneous catalysis would be the alternative biodiesel synthetic pathways since both conversion techniques are not susceptible to FFA and water content [30]. CTO contained a high percentage of UFA (77.12%) and low percentage of SFA (IV = 110.50 mg/gI$_2$). The SN of CTO appeared to be higher (150) than the AN (130). This could be attributed to the presence of TGs in CTO. Similar results were reported in the literature [31–34]. The CTO sample had a high amount of linoleic acid (46.24%) as compared to most of the reported results in the literature. Oleic acid was the predominant FFA in CTO in the studies by Jenab et al. [2] (47% of total FFA) and Demirbas [35] (39–49%). In accordance with our findings, linoleic acid was the FFA with the highest content in CTO, with 27.6% [15] and 19.1% [13]. The difference in the FA composition can be attributed to the fact that the extractable portion of wood components differs chemically from one wood species to another [34]. The presence of impurities, wood constituents and production method of CTO might all be a cause for the reported variability in the FA composition. Moreover, the unknown (unresolved) peaks in the FA chromatogram may likely represent impurities in the sample since CTO is a by-product from the Kraft pulping that is recovered through a set of complex operations that include concentration, skimming and acidulation of the black liquor soap [34,36].

4.2. Rheological Properties

In general, viscosity of tall oil responded in inverse proportionality to the shear rate and temperature, but was more dependent on the latter, as can be seen from the viscosity values at 30 °C and 40 °C (Figure 2). Data on the rheological flow properties of CTO were obtained by linearly increasing the shear rate from 50 to 250 s^{-1}. During the model analysis, five flow model types (Newtonian, Bingham, Casson, Power law, and Herschel–Bulkley) were fitted to the flow data. In the temperature range of 30–60 °C, the best-fitted model to the flow data was Herschel–Bulkley with a significant coefficient of determination. The results of the best-fitted flow model proved CTO as a non-Newtonian fluid within the selected temperatures range. Up to 40 °C, CTO had higher G″ values than G′ values, thereafter, G′ remained unchanged while G″ gradually declined until the end of the run. The intercepting point of G′ and G″ at 40 °C signified the glass transition temperature of CTO. The glass-transition temperature of a material characterizes a reversible transition in semi-crystalline materials from a hard and relatively tarlike state into a molten or rubberlike state. CTO displayed higher G″ than G′ values, up to 3 Hz, beyond which G′ grew exponentially whereas G″ increased linearly up to the end of the run. This result implied that CTO behaves as a strong viscoelastic liquid structure when the loss modulus (G") is lower than the storage modulus (G′), throughout the measured frequency range at 30 °C. The results obtained have provided useful information on important flow parameters of CTO for biodiesel production. The transition temperature, viscosity and viscoelastic behaviors of CTO have been clearly demonstrated. The selection of adequate operating temperature and, most importantly, best agitation intensity to

enhance biodiesel production from CTO has been deduced. To the best of our knowledge, this is the first report on rheological flow models of CTO.

4.3. Thermal Characteristics of CTO

The melting and crystallization are two major characteristics of the thermal properties of lipid-containing materials. As CTO is a complex by-product which contains a mixture of long-chain FA, RA, and neutral products. These CTO constituents play a major role in its thermal properties. Although many researchers have investigated the thermal properties of edible and non-edible vegetable oils and animal fats [16,21,37], there is limited information on the thermal properties of CTO available in the literature. To the best of our knowledge, this is the first time the thermal parameters of CTO are presented in a comprehensive and informative manner.

The chemical structure and physical properties of vegetable oil esters were correlated by Rodrigues et al. [38]. The authors concluded that the viscosity and crystallization temperature of vegetable oils are influenced by the degree of FA unsaturation. They further reported that a high concentration of UFA in vegetable oils lowers the crystallization temperature, regardless of the number of double bonds. In saturated TGs, the acyl chains can perfectly align along their chain length, which strengthens and maximizes the intermolecular interactions. Thus, more energy is needed to disintegrate the molecular association, which results in melting or molecular movement. The high crystallization value of CTO might be due to the presence of RA and sterols in it. The T_{onset} and T_{peak} at the crystallization and melting point of CTO have been shown to correlate to the rheological behavior of CTO.

The FA crystallization temperature appears to be a function of the length of the carbon chain and interactions between the molecules [38]. In a mixture of FAs, SFAs crystallize at higher temperatures than UFAs as SFAs have significantly higher melting points than UFAs. In the study of Wang et al. [39] on the rheological and thermal properties of soybean oils, the authors reported that oils rich in oleic acid and oils with low SFA content had a different DSC profile compared to other oils. Barba et al. [40] studied the crystallization and melting properties of extra virgin olive oil using synchrotron *X*-ray diffraction and DSC. Rodrigues et al. [38] also correlated the chemical structure and physical properties of vegetable oil esters and concluded that the viscosity and crystallization temperature of vegetable oils are influenced by the degree of FFA unsaturation. They further reported that a high concentration of UFA in vegetable oils lowers the crystallization temperature, regardless of the number of double bonds. When the FFA molecules are less saturated, they interact with each other primarily through Van der Waals bonding which can be easily disrupted at the solid–liquid transition [38].

5. Conclusions

This study revealed the thermal and rheological behavioral patterns of CTO at different shear rates and temperatures. The transesterification operating temperature for CTO as a biodiesel feedstock must exceed the temperature at which the viscosity becomes steady. Steady viscosity equally exists at a shear rate where an increase in the shear rate has no effect on the CTO viscosity. This information can be used to select appropriate agitation conditions for biodiesel production from CTO. If agitation is lowered or stopped at a shear rate corresponding to a steady viscosity, the transesterification reaction can proceed without any loss of biodiesel yield. This will, in turn, reduce wear and tear, as well as production cost. It was established that impurities in CTO can significantly influence the physicochemical properties, rheological behavior, and thermal properties of CTO. This information is useful for an adequate design of an optimal biodiesel production process and related processing equipment. Due to the high FA content, alkaline transesterification cannot be applied directly for biodiesel production without a preceding acid pretreatment step to reduce the FA levels in CTO first. Alternatively, a heterogeneous catalysis or enzyme-catalyzed transesterification would be viable biodiesel production options that do not require prior modification of the FA content in CTO.

Author Contributions: P.A and L.C conceived and designed the experiments; P.A performed the experiments, analyzed the data and wrote the paper; L.C reviewed the paper before submission.

Conflicts of Interest: The authors declare no conflict of interest. The funding sponsors had no role in or contribution to the design and performance of research experiments, data analysis and interpretation, manuscript preparation and publication.

References

1. Mäki-Arvela, P.; Mikkola, M.; Hemming, J.; Eränen, K.; Willför, S.; Murzin, D.Y. Heat Treatment and Chemical Composition of Fatty Acids and Rosin Acids Mixtures: Effects on Their Thermal Properties and Morphology. *J. Am. Oil Chem Soc.* **2014**, *91*, 1035–1046. [CrossRef]

2. Jenab, E.; Mussone, P.; Nam, G.; Bressler, D. Production of Renewable Hydrocarbons from Thermal Conversion of Abietic Acid and Tall Oil Fatty Acids. *Energy Fuels* **2014**, *28*, 6988–6994. [CrossRef]

3. Mäki-Arvela, P.; Holmbom, B.; Salmi, T.; Murzin, D.Y. Recent Progress in Synthesis of Fine and Specialty Chemicals from Wood and Other Biomass by Heterogeneous Catalytic Processes. *Catal. Rev.* **2007**, *49*, 197–340. [CrossRef]

4. Valto, P.; Knuutinen, J.; Alén, R. Overview of analytical procedures for fatty and resin acids in the papermaking process. *BioResources* **2012**, *7*, 6041–6076. [CrossRef]

5. Yakushin, V.; Stirna, U.; Bikovens, O.; Misane, M.; Sevastyanova, I.; Vilsone, D. Synthesis and Characterization of Novel Polyurethanes Based on Tall Oil. *Mater. Sci.* **2013**, *19*, 390–396. [CrossRef]

6. Murillo, E.A.; Vallejo, P.P.; López, B.L. Effect of tall oil fatty acids content on the properties of novel hyperbranched alkyd resins. *J. Appl. Polym. Sci.* **2011**, *120*, 3151–3158. [CrossRef]

7. Liu, K.; Madbouly, S.A.; Schrader, J.A.; Kessler, M.R.; Grewell, D.; Graves, W.R. Biorenewable polymer composites from tall oil-based polyamide and lignin-cellulose fiber. *J. Appl. Polym. Sci.* **2015**, *132*, 1–9. [CrossRef]

8. Bocqué, M.; Voirin, C.; Lapinte, V.; Caillol, S.; Robin, J.-J. Petro-based and bio-based plasticizers: Chemical structures to plasticizing properties. *J. Polym. Sci. Part A* **2016**, *54*, 11–33. [CrossRef]

9. Ikladious, N.E.; Mansour, S.H.; Asaad, J.N.; Emira, H.S.; Hilt, M. Synthesis and evaluation of new hyperbranched alkyds for coatings. *Prog. Org. Coat.* **2015**, *89*, 252–259. [CrossRef]

10. Murillo, E.A.; Vallejo, P.P.; López, B.L. Synthesis and characterization of hyperbranched alkyd resins based on tall oil fatty acids. *Prog. Org. Coat.* **2010**, *69*, 235–240. [CrossRef]

11. Mkhize, N.M.; Sithole, B.B.; Ntunka, M.G. Heterogeneous Acid-Catalyzed Biodiesel Production from Crude Tall Oil: A Low-Grade and Less Expensive Feedstock. *J. Wood Chem. Technol.* **2015**, *35*, 374–385. [CrossRef]

12. Demirbas, A. Methylation of wood fatty and resin acids for production of biodiesel. *Fuel* **2011**, *90*, 2273–2279. [CrossRef]

13. Anthonykutty, J.M.; Linnekoski, J.; Harlin, A.; Laitinen, A.; Lehtonen, J. Catalytic upgrading of crude tall oil into a paraffin-rich liquid. *Biomass. Convers. Biorefinery* **2014**, *5*, 149–159. [CrossRef]

14. Coll, R.; Udas, S.; Jacoby, W.A. Conversion of the Rosin Acid Fraction of Crude Tall Oil into Fuels and Chemicals. *Energy Fuels* **2001**, *15*, 1166–1172. [CrossRef]

15. De Bruycker, R.; Anthonykutty, J.M.; Linnekoski, J.; Harlin, A.; Lehtonen, J.; Van Geem, K.M.; Räsänen, J.; Marin, G.B. Assessing the Potential of Crude Tall Oil for the Production of Green-Base Chemicals: An Experimental and Kinetic Modeling Study. *Ind. Eng. Chem. Res.* **2014**, *53*, 18430–18442. [CrossRef]

16. Adewale, P.; Dumont, M.-J.; Ngadi, M. Rheological, Thermal, and Physicochemical Characterization of Animal Fat Wastes for use in Biodiesel Production. *Energy Technol.* **2014**, *2*, 634–642. [CrossRef]

17. Karmakar, A.; Karmakar, S.; Mukherjee, S. Properties of various plants and animals feedstocks for biodiesel production. *Bioresour. Technol.* **2010**, *101*, 7201–7210. [CrossRef] [PubMed]

18. Alicke, A.A.; Leopércio, B.C.; Marchesini, F.H.; de Souza Mendes, P.R. Guidelines for the rheological characterization of biodiesel. *Fuel* **2015**, *140*, 446–452. [CrossRef]

19. Aguirre-Mandujano, E.; Lobato-Calleros, C.; Beristain, C.I.; Garcia, H.S.; Vernon-Carter, E.J. Microstructure and viscoelastic properties of low-fat yoghurt structured by monoglyceride gels. *LWT - Food Sci. Technol.* **2009**, *42*, 938–944. [CrossRef]

20. Liu, C.; Yang, M.; Huang, F. Influence of Extraction Processing on Rheological Properties of Rapeseed Oils. *J. Am. Oil Chem. Soc.* **2012**, *89*, 73–78. [CrossRef]

21. Abdul Azis, A.; Mohamud, Y.; Roselina, K.; Che Man, Y.B.; Boo, H.C.; Nyuk, L.C. Rheological, chemical and DSC thermal characteristics of different types of palm oil/palm stearin-based shortenings. *Int. Food Res. J. Int. Food Res.* **2011**, *18*, 189–200.

22. Tan, C.; Man, Y. Comparative differential scanning calorimetric analysis of vegetable oils: I. Effects of heating rate variation. *Phytochem. Anal.* **2002**, *13*, 129–141. [CrossRef] [PubMed]

23. Atabani, A.E.; Mahlia, T.M.I.; Anjum Badruddin, I.; Masjuki, H.H.; Chong, W.T.; Lee, K.T. Investigation of physical and chemical properties of potential edible and non-edible feedstocks for biodiesel production, a comparative analysis. *Renew. Sustain. Energy Rev.* **2013**, *21*, 749–755. [CrossRef]

24. Ma, F.; Clements, L.; Hanna, M. The Effects of Catalyst, Free Fatty Acids, and Water on Transecterification of Beef Tallow. *Trans. ASAE* **1998**, *41*, 1261–1264. [CrossRef]

25. Balo, F. Feasibility study of "green" insulation materials including tall oil: Environmental, economical and thermal properties. *Energy Build.* **2015**, *86*, 161–175. [CrossRef]

26. Canoira, L.; Rodríguez-Gamero, M.; Querol, E.; Alcántara, R.N.; Lapuerta, M.N.; Oliva, F.N. Biodiesel from Low-Grade Animal Fat: Production Process Assessment and Biodiesel Properties Characterization. *Ind. Eng. Chem. Res.* **2008**, *47*, 7997–8004. [CrossRef]

27. Ramírez-Verduzco, L.F.; Rodríguez-Rodríguez, J.E.; Jaramillo-Jacob, A.D.R. Predicting cetane number, kinematic viscosity, density and higher heating value of biodiesel from its fatty acid methyl ester composition. *Fuel* **2012**, *91*, 102–111. [CrossRef]

28. Canakci, M.; Van Gerpen, J. A pilot plant to produce biodiesel from high free fatty acid feedstocks. *Trans. ASAE* **2003**, *46*, 945–954. [CrossRef]

29. Canakci, M. The potential of restaurant waste lipids as biodiesel feedstocks. *Bioresour. Technol.* **2007**, *98*, 183–190. [CrossRef] [PubMed]

30. Adewale, P.; Dumont, M.-J.; Ngadi, M. Recent trends of biodiesel production from animal fat wastes and associated production techniques. *Renew. Sustain. Energy Rev.* **2015**, *45*, 574–588. [CrossRef]

31. Keskin, A.; Gürü, M.; Altıparmak, D. Biodiesel production from tall oil with synthesized Mn and Ni based additives: Effects of the additives on fuel consumption and emissions. *Fuel* **2007**, *86*, 1139–1143. [CrossRef]

32. Keskin, A.; Gürü, M.; Altıparmak, D. Influence of tall oil biodiesel with Mg and Mo based fuel additives on diesel engine performance and emission. *Bioresour. Technol.* **2008**, *99*, 6434–6438. [CrossRef] [PubMed]

33. Altıparmak, D.; Keskin, A.; Koca, A.; Gürü, M. Alternative fuel properties of tall oil fatty acid methyl ester–diesel fuel blends. *Bioresour. Technol.* **2007**, *98*, 241–246. [CrossRef] [PubMed]

34. Norlin, L.H. Tall oil. In *Ullmann's Encyclopedia of Industrial Chemistry*; John Wiley and Sons, Inc.: Somerset, NJ, USA; Wiley-VCH Verlag GmbH & Co. KGaA: Weinheim, Germany, 2000; pp. 583–596.

35. Demirbas, A. Production of Biodiesel from Tall Oil. Energy Sources, Part A: Recovery, Utilization, and Environ. *Effects* **2008**, *30*, 1896–1902.

36. Panda, H. *Handbook on Tall Oil Rosin Production, Processing and Utilization*; Asia Pacific Business Press Inc.: Delhi, India, 2013.

37. Tan, C.; Che Man, Y. Differential scanning calorimetric analysis of edible oils: Comparison of thermal properties and chemical composition. *J. Am. Oil Chem. Soc.* **2000**, *77*, 143–155. [CrossRef]

38. Rodrigues, J.; Cardoso, F., Jr.; Lachter, E.; Estevão, L.M.; Lima, E.; Nascimento, R.V. Correlating chemical structure and physical properties of vegetable oil esters. *J. Am. Oil Chem. Soc.* **2006**, *83*, 353–357. [CrossRef]

39. Wang, T.; Briggs, J.L. Rheological and thermal properties of soybean oils with modified FA compositions. *J. Am. Oil Chem. Soc.* **2002**, *79*, 831–836. [CrossRef]

40. Barba, L.; Arrighetti, G.; Calligaris, S. Crystallization and melting properties of extra virgin olive oil studied by synchrotron XRD and DSC. *Eur. J. Lipid Sci. Technol.* **2013**, *115*, 322–329. [CrossRef]